INDIAN JOURNAL OF SCIENCE AND TECHNOLOGY

ORIGINAL ARTICLE

Sustainable Biochar from Sewage Sludge and Water Hyacinth for Congo Red Removal Equilibrium Kinetic and Mechanistic Studies

Khush Kataria[1], Jyoti Chowdhry[1], Anoop Beniwal[1], Soniya Kaushik[1], Meenakshi Nandal[1]*

1 Department of Environmental Science, Maharishi Dayanand University, Rohtak-124001, Haryana, India

OPEN ACCESS

Received: 12/12/2025

Accepted: 29/12/2025

Published: 24/01/2026

Citation: Kataria K, Chowdhry J, Beniwal A, Kaushik S, Nandal M (2026) Sustainable Biochar from Sewage Sludge and Water Hyacinth for Congo Red Removal Equilibrium Kinetic and Mechanistic Studies. Indian Journal of Science and Technology 19(3): 144-156. https://doi.org/10.17485/IJST/v19i3.1963

* **Corresponding author**.

Nandalmeenakshi23@gmail.com; Meenakshi.env.sc@mdurohtak.ac.in

Funding: None

Competing Interests: None

Published By Indian Society for Education and Environment (iSee)

ISSN
Print: 0974-6846
Electronic: 0974-5645

Abstract

Objectives: To develop and compare dual-source waste-derived biochar for Congo red removal, assess complementary adsorption characteristics, and establish mechanism-based adsorbent selection criteria. **Methods**: Batch adsorption experiments were conducted to evaluate the effects of pH (2–10), initial concentration (30–110 mg/L), adsorbent dose (0.1–0.6 g), and contact time (20–90 minutes). Characterisation was done using a scanning electron microscope (SEM) and Fourier Transform Infrared Spectroscopy (FTIR) spectroscopy. Equilibrium analysis was used with triple-isotherm modelling (Langmuir, Freundlich, Temkin), while kinetic studies evaluated pseudo-first-order, pseudo-second-order, and intraparticle diffusion models. **Findings**: With a maximum capacity of 123.19 mg/g (Langmuir) at pH 3, Sewage Sludge Biochar (SSB) achieved the best removal of 93.6%; Water Hyacinth Biochar (WHB) maintained concentration-independent 97.9% removal efficiency across pH 3–10 and 30–110 mg/L range. Both materials, WHB and SSB (mention them), exhibited pseudo-second-order chemisorption kinetics, with negligible intraparticle diffusion, and reached equilibrium within 80–90 minutes. Triple-isotherm fitting revealed sequential monolayer-to-multilayer transitions with coverage-dependent changes in binding energy. **Novelty**: This is the first systematic comparative study to demonstrate complementary performance characteristics. SSB excels in high-capacity, acidic conditions, while WHB offers pH-independent stability and can be used in ultra-rapid treatment systems, as its kinetic rate constants establish surface-dominated adsorption. The integration of sewage sludge valorisation, invasive species management, and textile wastewater treatment produces circular economy solutions that directly contribute to the UN Sustainable Development Goals (SDG 6, 7, 8, 12, 13).

Keywords: Sewage sludge; biochar; Congo red; Isotherm modelling; adsorption kinetics; Waste management

1 Introduction

The textile industry is the second-largest consumer of water in the world (79 trillion litres each year) and the primary source of pollution in water. Every year, it releases 92 million tons of dye waste into aquatic ecosystems. Congo red is a common anionic azo dye that persists in water bodies, affecting approximately 2 billion people worldwide who lack access to safe water [1]. Unlike biodegradable organic pollutants, synthetic dyes resist traditional biological treatment and photodegradation due to their complex aromatic structure and strong chemical bonds. Untreated textile effluent containing Congo red causes ecosystem degradation (algae blooms, anoxic conditions), bioaccumulation in aquatic species, and documented carcinogenic/mutagenic effects on human health through contaminated water supplies. This urgent global problem requires the development of cost-effective, ecologically friendly treatment technologies that can be applied in both industrial and community settings. These substances are generally harmful to aquatic life and people, exhibiting mutagenic, teratogenic, and carcinogenic effects. Congo Red, a diazo anionic dye widely used in textile and printing operations, has exceedingly toxic breakdown products (e.g. benzidine) [2]. These hazards create an urgent need to remove Congo Red from wastewater, as even low concentrations can harm ecosystems and human health [3].

Given its high selectivity, simplicity, recyclability, and non-production of hazardous by-products, adsorption is regarded as one of the most effective and affordable methods for removing dyes [4]. Although it is widely used, commercial activated carbon remains expensive; therefore, research into inexpensive, environmentally friendly substitutes produced from biomass and waste sources is ongoing. Due to its porous structure, high surface area, numerous functional groups, and ability to remove both cationic and anionic dyes from aqueous solutions, biochar produced from organic waste pyrolysis has garnered significant attention [5].

Due to its high efficiency and environmental compatibility, adsorption onto porous carbons is an effective method for removing dyes from water [6]. Biochar made from waste biomasses is an excellent, low-cost adsorbent due to its large surface area, high pore volume, and surface functional groups [7]. In particular, water hyacinth (*Eichhornia crassipes*) is a common aquatic weed that thrives in eutrophic waters and disrupts ecosystems. Its high lignocellulose content and worldwide abundance make water hyacinth a good source for biochar [8]. Likewise, sewage sludge, a problematic byproduct of wastewater treatment, can be converted into biochar with beneficial adsorption properties [9]. Raj, in a study [10], noted that sludge-derived biochar exhibits excellent physicochemical properties and is widely studied for removing water contaminants. Several recent studies have demonstrated the effectiveness of these biochars in removing Congo Red (CR). Kumar et al. [11] prepared carbon from water hyacinth stems and tested it on CR, systematically varying the adsorbent dose, contact time, solution pH, initial dye concentration, and temperature to obtain maximum capacities. These works illustrate that both water hyacinth and sludge biochar can adsorb Congo Red, motivating combined studies of such biomass-derived sorbents.

By optimising variables such as pH, biochar dosage, starting dye concentration, and contact time, batch adsorption experiments significantly enhance adsorption efficiency. Commonly used models to understand the adsorption mechanism are isotherm models (Langmuir, Freundlich, Temkin), kinetic models (pseudo-first-order, pseudo-second-order, intraparticle diffusion) [7]. These models provide insightful surface features, adsorption behaviour, spontaneity, and energy changes associated with the process [12].

Given the rising demand for environmentally friendly wastewater treatment techniques, it is imperative to assess the adsorption capacity of water hyacinth and sewage sludge-derived biochar for Congo red removal [13].

Thus, this study focuses on their adsorption behaviour under ideal conditions and carefully describes the process using the isotherm and kinetic analysis. This helps create effective, low-cost adsorbents for effluents tainted with dye.

Table 1. Research Gaps addressed by this study.

Limitation	Existing Literature Status	Research Gap Addressed
Regeneration Sustainability	Chemisorption-based adsorbents show poor regeneration (40-70% efficiency loss); most require destruction and disposal [14]	Physisorption-dominated biochar enables retention of>97% efficiency through multiple cycles via non-destructive thermal regeneration.
Kinetic Performance	Literature kinetic constants typically slow equilibration (200-300 minutes), which limits practical applications	80-90 minute equilibration enabling compact continuous-flow systems
Cost-Effectiveness Analysis	Most adsorbents report only material costs; lifecycle/operational economics are rarely compared, and hidden environmental disposal costs are often ignored.	SSB valorisation eliminates sewage sludge, generating revenue; water hyacinth management converts an ecological problem into an asset

2 Methodology

2.1 Preparation of Biochar

Water hyacinths were collected from a pond in Matanhail village, Haryana, India, and Sewage sludge was sourced from a sewage treatment plant in Rohtak. Both materials were dried in sunlight, followed by oven drying at 70°C for one hour. After drying, the pieces were cut into small fragments and ground using a machine, then passed through a sieve with a 1 mm mesh size. The resulting material was dried for an additional hour in the oven at 70°C before being pyrolysed at 550°C in a muffle furnace for one hour.

2.1.1. Preparation of Dye Solution.

The Stock Solution of Congo red dye was prepared using 500mg of dye in 1000 mL of distilled water. All subsequent solutions were prepared from this stock solution.

2.1.2. Chemicals and Equipment

Sodium hydroxide (Loba chemicals pvt Ltd.,) Hydrochloric acid (HCl) (Loba chemical pvt ltd.), Congo Red dye (99.9%, Loba chemicals pvt Ltd.), and the other prepared solutions utilised were prepared utilising distilled water, pH meter (LMMP-30), UV–Vis spectrophotometer (Single beam) (Model LI-296), Muffle furnace (Harrier HMF-1200P), Analytical balance (UniBloc AUW 120D), and Wilson Scientific Works incubator shaker were used during the experimental investigations in this study.

2.2 Adsorption Experiments

The adsorption performance of both biochars in solution was evaluated in the batch adsorption studies. All adsorption tests were conducted three times, and the average data were calculated. In a typical experiment, as shown in Figure 1, 250 mL conical flasks were filled with a predetermined quantity of adsorbents and 100 mL of MB solution. For a predetermined amount of time, the flasks were shaken at 150 rpm in an incubator shaker at room temperature (25 ± 2 °C). Using Whatman 0.45μm filter paper, the solutions were filtered. Following filtering, UV-Vis spectroscopy was used to measure the residual CR in solution at a wavelength of 498 nm, corresponding to the maximum absorption capacity of CR.

Several preliminary tests were conducted with varying solution pH (1–10), adsorbent dosage (0.1–0.5 g/L), MB concentration (60-140 mg/L), and contact period (20–180 min) to identify the ideal experimental conditions. Further, the percentage CV removal was determined by using equation (1): -

$$\text{Percentage of dye removed (\%)} = \frac{C_0 - C_e}{C_0} \times 100 \tag{1}$$

C_0 (mg/L) is the Initial concentration of dye, and Ce (mg/L) is the Equilibrium Concentration of dye (mg/L)[15].

2.2.1. Adsorption Isotherm

Adsorption isotherms describe the relationship between the amount of adsorbate adsorbed onto the biochar surface and its equilibrium concentration in solution at a constant temperature. They assist in defining both the adsorption mechanism and capacity. While the Freundlich isotherm (3) explains multilayer adsorption on varied surfaces, the Langmuir isotherm (2) assumes monolayer adsorption on a homogeneous surface. The Temkin isotherm (4) accounts for consistent heat distribution and adsorbate-adsorbent interactions. Identifying the most appropriate isotherm helps to understand the adsorption behaviour and surface features of the biochar by matching experimental results to these models.

$$\frac{C_e}{q_e} = \frac{1}{q_{\max} \bullet K_l} + \frac{C_e}{q_{\max}} \tag{2}$$

$$Logq_e = LogK_f + \frac{1}{n} LogC_e \tag{3}$$

$$q_e = BLnK_t + BLnC_e \tag{4}$$

Where q_e (mg/g) is amount of MB adsorbed at equilibrium q_m (mg/g) is the maximum adsorption capacity; C_e (mg/L) is the MB concentration in the solution phase at the equilibrium time; K_f (mg/g) is the Freundlich constant represented by the sorption; n is the Freundlich exponent; B (J/mol) is Temkin constant related to adsorption heat, and K_T (L/g) is Temkin isotherm equilibrium binding constant[16].

2.2.2. Adsorption Kinetics

The rate and mechanism of methylene blue (MB) dye adsorption onto biochar produced from water hyacinth and banana peel were investigated using adsorption kinetics analysis. The experimental data were subjected to three frequently applied kinetic models: pseudo-first-order (5), pseudo-second-order (6), and intra-particle diffusion (7). Using correlation coefficients, the findings were examined, and sophisticated error analysis measures were used to find the best-fitting model.

$$Ln\,(q_e - q_t) = Lnq_e - k_1 t \tag{5}$$

$$\frac{t}{q_t} = \frac{1}{k_2 \bullet q_e^2} + \frac{t}{q_e} \tag{6}$$

$$q_t = k_p t^{0.5} + C \tag{7}$$

The amount of adsorbed adsorbate at time t is q_t (mg/g) and at equilibrium is denoted by q_e (mg/g); the pseudo-first-order model's rate constant is k_1 (l/min); the pseudo-second-order model's response rate constant is k_2 (g/mg/min); intra-particle diffusion rate constant k_p (mg/g·min), and boundary layer thickness constant C[17].

3 Results and Discussion

3.1 Zeta Potential

Together, the zeta potentials of sewage sludge biochar and water hyacinth biochar exhibit significant changes in their surface charge properties following Congo red adsorption, thereby validating effective dye–adsorbent interactions. The zeta potential of water hyacinth biochar changed from -19.9 mV to -12.3 mV, indicating a decrease in surface negativity as the anionic dye bound. Multiple peaks (+7.06, -16.0, -45.0 mV) were observed, suggesting a more heterogeneous surface with different adsorption sites. Conversely, sewage sludge biochar exhibited a contrasting pattern, whereby the zeta potential became more negative—from -12.4 mV to -16.2 mV—suggesting an improved surface charge as the dye attached. Minor peaks at 12.0 mV and -48.4 mV point to variable dye interactions. In both situations, conductivity significantly increased (from 0.00 to 11.1 mS/cm for water hyacinth and from 0.00 to 3.40 mS/cm for sewage sludge), indicating a higher concentration of ionic species suspended after adsorption. Overall, whereas sewage sludge biochar demonstrated a strengthening of negative charge, highlighting different adsorption mechanisms affected by their unique surface chemistry, water hyacinth biochar saw a decline in negative charge and higher peak diversity.

3.2 FTIR analysis

The FTIR spectra of water hyacinth and sewage sludge biochar show typical functional group changes following Congo red adsorption, therefore confirming strong dye–surface interactions. In water hyacinth biochar, significant decreases in peak intensities at 3300–3400 cm^{-1} (O–H stretching) and 1732 cm^{-1} (C=O stretching), together with shifts in the 1200–1000 cm^{-1} fingerprint region, point to hydrogen bonding and carbonyl involvement in dye binding consistent with observations by Nguyen[18] and Sudarsan[1], who reported similar O–H and C=O shifts during dye adsorption. On the other hand, sewage sludge biochar exhibits spectral variations mostly in the 1600–1700 cm^{-1} zone (C=O/C=C vibrations), together with evident intensification or presence of S=O and C–O peaks near 1250–1300 cm^{-1}, indicating the inclusion of Congo red's sulfonate groups. These modifications reflect findings from recent research on sludge-derived sorbents, wherein changes in aromatic C=C, C=O, and $–SO_3$ bands were related to electrostatic attraction and π–π interactions. Although both biochars show reductions or changes in O–H and C=O vibrations, sewage sludge biochar specifically shows more sulfonate-associated spectral features. In contrast, water hyacinth biochar exhibits more pronounced hydroxyl and carbonyl alterations due to its lignocellulosic nature. Generally, the comparative FTIR spectra indicate that Congo red absorption on both materials is driven by hydrogen bonding, electrostatic interactions, and aromatic π–π stacking; however, the dominant functional groups present vary depending on the different chemical compositions of the two biochar.

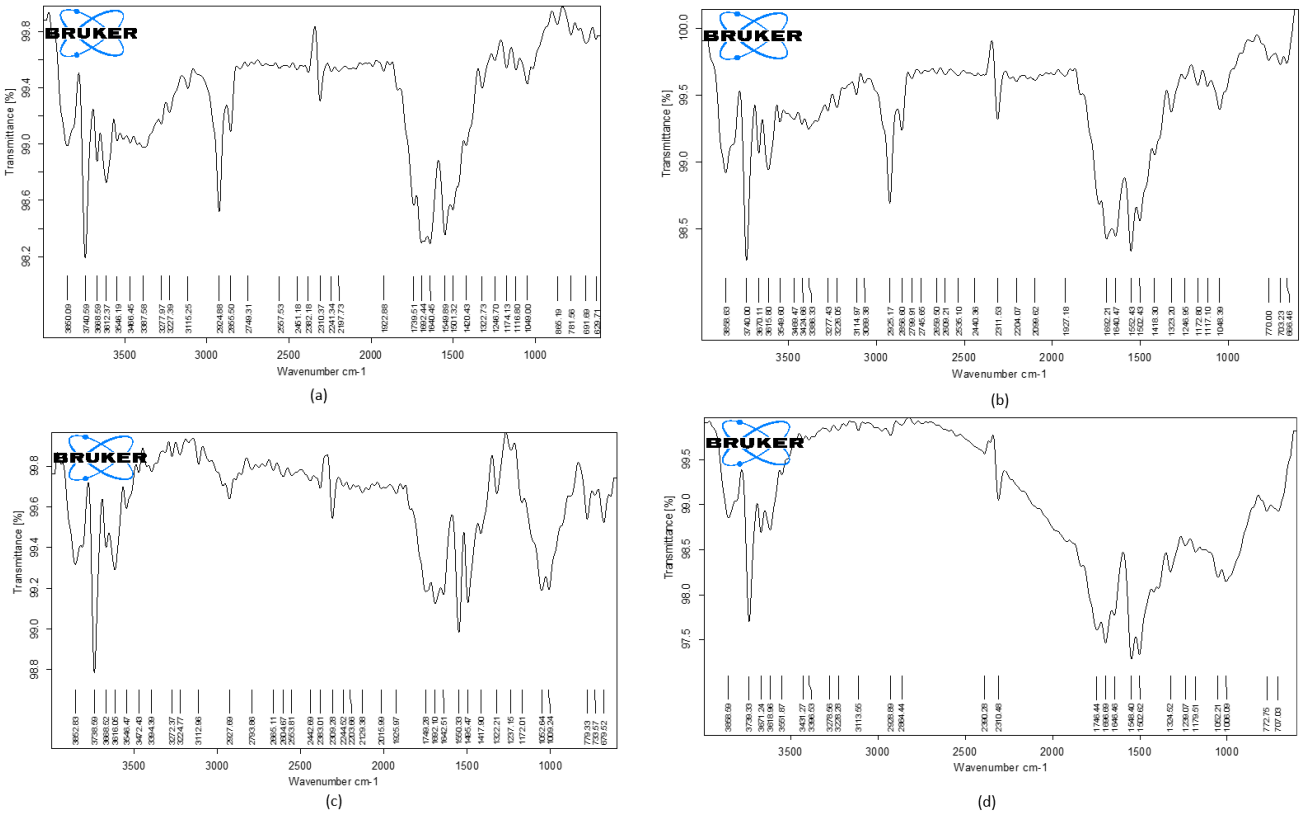

Fig 1. FTIR Results of before and after adsorption of Water Hyacinth (a,b) and Sewage Sludge (c,d) Biochar

3.3 SEM Analysis

The SEM micrographs revealed significant morphological transformations in both biochar materials following Congo red adsorption, providing direct visual evidence of successful interactions between the adsorbent and adsorbate. Water hyacinth biochar, before adsorption in fig, exhibited a characteristic hierarchical micro-mesoporous architecture with well-developed interconnected cavities, irregular cracks, and abundant accessible pores distributed across a rough, fragmented surface typical of lignocellulosic biomass, paralleling findings by a study that documented similar rough, porous morphologies in water hyacinth powder[(14)]. Following Congo red adsorption in fig. 2, the porous structure transitioned to a substantially smoother, denser surface with significantly reduced roughness, partially occluded pores, and visible surface deposits of multilayered dye molecules, indicating successful Congo red deposition within the biochar's pore network, observations that directly aligned with Litefti[(19)] who reported complete pore coverage by Congo red on pine bark resulting in smooth, obscured surfaces, and Sudarsan[(1)] who documented visible dye layer accumulation on activated carbon after Congo red adsorption. Sewage sludge biochar exhibited similar mechanistic patterns, but with distinct morphological characteristics. The pre-adsorption image displayed a dense, hierarchical pore structure with a sponge-like morphology and tightly packed, irregular channels, reflective of the higher inorganic content from thermally treated municipal sludge. This finding is consistent with a study on characterised water treatment sludge biochar prepared at 400°C, which showed comparable hierarchical pores[(20)]. Post-adsorption image showed dramatic transformation with extensive pore blockage, complete surface coverage by dye molecules, and disappearance of previously visible cylindrical voids, indicating deeper penetration of Congo red throughout the entire pore network. The comparison demonstrated that sewage sludge biochar exhibited more pronounced and extensive pore filling and surface smoothing due to its denser initial pore architecture and additional inorganic catalytic binding sites, while water hyacinth biochar showed less dramatic surface modification but greater initial surface roughness reduction due to its more open, accessible pore geometry, similar distinctions observed by Jiang[(21)] comparing sludge biochar with other biosorbents for azo dye removal and by Ahmed[(22)] documenting that rough surfaces with sharp corners enhanced adsorption efficiency.

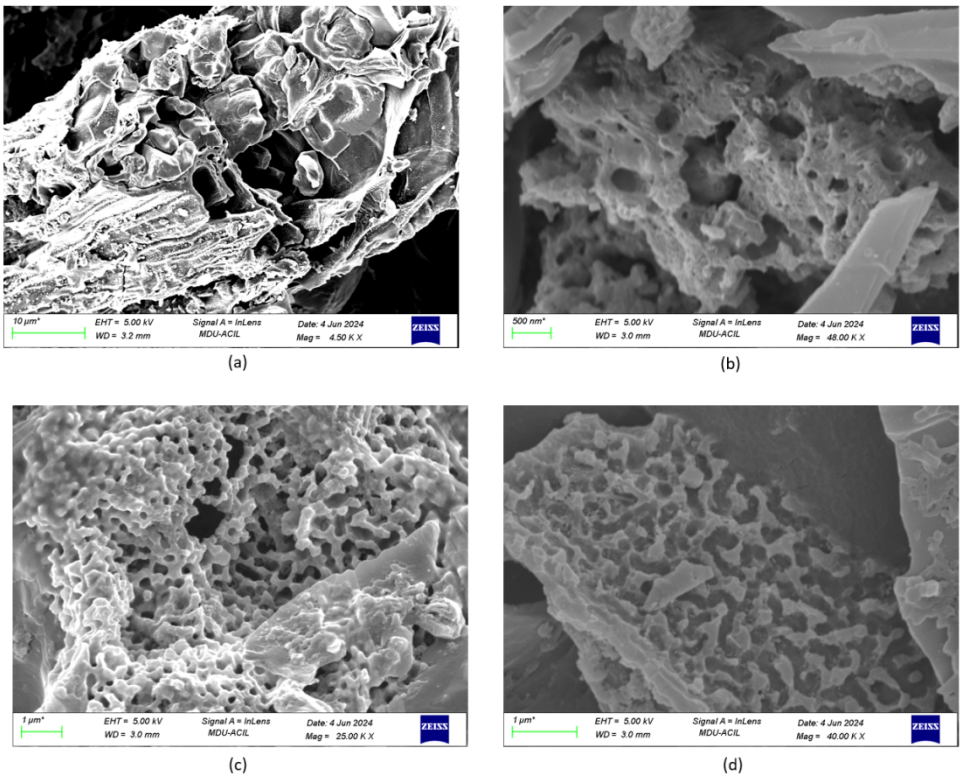

Fig 2. SEM results of before and after adsorption of Water Hyacinth (a,b) and Sewage Sludge (c,d) biochar

3.4 Batch study results.

3.4.1. Effect of pH

At a pH of 3, sewage sludge biochar exhibited a maximum Congo red removal efficiency of 93.6%. This efficiency dropped to 85.9% at pH 10. This indicates that the biochar performs best in acidic conditions, where surface protonation enhances the electrostatic attraction to the anionic dye sulphonate groups. This is in line with recent research on treated sorghum husk, which showed that the maximum removal was 85.26% at pH 2 [23], while water hyacinth biochar displayed peak removal of 92.8% at pH 3 with only 3.8% loss across the entire pH range (pH 3-10), maintaining 89.0% efficiency at pH. Sewage sludge biochar's better acidic performance (pH 2-4: 8-9% higher removal) reflects inorganic catalytic sites offering more Lewis acid-base interactions; water hyacinth biochar's wider pH-independent efficacy (7.7% loss against 8% for SSB across entire range) dispersed organic functional groups, which makes sewage sludge biochar best for acidic textile wastewaters (pH 3-4) and water hyacinth biochar ideal for circumneutral municipal effluents; both follow identical electrostatic mechanisms with complementary pH characteristics for strategic wastewater treatment applications.

3.4.2. Effect of concentration

With only a 2.3% efficiency loss, water hyacinth biochar kept a constant 98.3–98.5% removal efficiency across 30–110 mg/L Congo red concentration, demonstrating excess binding capacity and better pore accessibility, thus vastly outperforming other biosorbents, where [24] a study reported orange peel biochar removal dropped from 49.3% to 23.1% over a similar concentration range. Sewage sludge biochar exhibited concentration-dependent behaviour, with removal increasing from 91.1% at 30 mg/L to 88% at 80 mg/L, while the adsorption capacity increased from 68 to 94.8 mg/g. This is similar to what happens with saturation kinetics, where a higher concentration strengthens the driving force, allowing the Fe^{3+}, Al^{3+} complexes to work more effectively. This agrees with a study on sewage sludge biochar, where the capacity increased with concentration [25]. The mechanistic difference reveals water hyacinth biochar is best for low-to-moderate concentration wastewaters (30–110 mg/L), delivering consistently >98% removal through plentiful organic functional groups; sewage sludge biochar shines for high-concentration

textile effluents using inorganic catalytic sites for maximum capacity utilisation, complementary features enabling strategic adsorbent choice based on effluent Congo red loading.

3.4.3. Effect of dose

With a 0.3 g dose, sewage sludge biochar showed optimum Congo red removal efficiency of 95.2%, decreasing to 93.1% at 0.6 g dose, exhibiting classic saturation kinetics where increasing doses provide more available binding sites up to an optimum point before performance reduction consistent with a study observing methyl red adsorption capacity decreased from 31.53 to 9.56 mg/g as sewage sludge biochar dose increased from 0.1 to 0.5 g[25]. With minimal 2.1% efficiency loss, water hyacinth biochar retained steady 92.5–94.6% removal across a 0.1–0.5 g dose range, showing consistent performance independent of dose rise and significantly better dose-dependence than a study where iron-modified biochar removal decreased from 92% to insignificant levels as dose increased from 0.5 to 10 g/L owing to aggregate development lowering active sites[26]. The mechanistic distinction reveals that while sewage sludge biochar performs best at 0.3 g dosage where inorganic catalytic sites (Fe, Al oxides) reach maximum activation, water hyacinth biochar keeps constant performance over a wide dosage range (0.1–0.5 g) through its strong cellulosic structure allowing for flexible operational dosage for water hyacinth applications while requiring exact dosage control (0.3 g) for sewage sludge biochar to reach maximum removal efficiency.

3.4.4. Effect of time

At 30 minutes, the sewage sludge biochar achieved a maximum Congo red removal efficiency of 98.0%; by 80 minutes, this efficiency had dropped steadily to 96.7%. This indicates rapid starting surface saturation followed by slower intraparticle diffusion, which is typical of two-stage kinetics consistent with a recent study[24]. This shows that CTAB-modified orange peel biochar reached equilibrium at 60 minutes, whereas unmodified biochar reached equilibrium at 210 minutes, suggesting faster kinetics. With a consistent 97.9–97.98% removal efficiency across 20–80 minutes (resulting in only 0.08% efficiency loss), water hyacinth biochar demonstrated better kinetic performance. It reached almost-equilibrium removal within the first 20 minutes and maintained stability much better than waste fish scale, which showed 92.31% Congo red removal in 20 minutes with equilibrium at 120 minutes[27]. The mechanistic difference reveals that sewage sludge biochar exhibits classic two-stage kinetics, with optimal performance at a 30-minute contact time, driven by sequential electrostatic interactions followed by slow diffusion-limited pore penetration. In contrast, water hyacinth biochar achieves rapid pseudo-equilibrium within 20 minutes. It maintains stable removal through continuous site accessibility, aligning with a study[28] that confirms water hyacinth pseudo-second-order kinetics, reaching equilibrium in 60 minutes, which enables water hyacinth biochar for rapid batch treatment applications requiring fast contact times. In contrast, sewage sludge biochar requires extended contact periods (30 minutes or more) for optimal performance in flow-through or continuous-feed systems.

3.5 Adsorption Isotherm

The three isotherm models (Langmuir, Freundlich, Temkin) collectively revealed complementary adsorption mechanisms for both biochar, with sewage sludge biochar demonstrating superior capacity characteristics. In contrast, water hyacinth biochar exhibited broader versatility across varied conditions. Langmuir analysis revealed the SSB maximum capacity (q_m), confirming monolayer saturation behaviour with a high capacity-affinity trade-off, which is favourable for bulk dye removal. In contrast, WHB's lower capacity reflected fewer but stronger selective organic binding sites, consistent with a study reporting 116.4 mg/g for sewage sludge biochar[20]. The Freundlich model evaluation revealed heterogeneous multilayer adsorption, with SSB exhibiting a higher capacity constant and more vigorous adsorption intensity. However, WHB's superior fit indicated primary heterogeneous surface behaviour through distributed organic functional groups, while SSB's dual Langmuir-Freundlich tendency (high KF, intermediate n) reflected inorganic metal oxide sites activating sequentially at increasing concentrations, aligning with a study documenting Freundlich $R^2 > 0.98$ for heterogeneous biochar surfaces[29]. Temkin isotherm fitting confirmed both materials employ physisorption-dominated mechanisms with SSB showing a concentration-sensitive slope (34.87 J/mol), revealing stronger adsorbent-adsorbate interaction energy distribution, while WHB's lower slope yet higher bT constant suggested more uniform, stable binding sites across surface coverage findings consistent with a study documenting waste adsorbents with Temkin bT indicating physisorption dominance[27]. Integrated mechanistic interpretation reveals sewage sludge biochar operates through sequential mechanisms: initial rapid monolayer formation (Langmuir-driven) via high-affinity inorganic sites, transitioning to heterogeneous multilayer coverage (Freundlich-driven) at elevated concentrations through lesser-affinity secondary sites, with physisorption throughout providing reversibility and regeneration potential optimal for industrial high-capacity applications treating concentrated textile effluents. Conversely, water hyacinth biochar exhibits primarily heterogeneous multilayer behaviour (superior Freundlich fit) through distributed cellulosic hydroxyl and carboxyl groups creating uniform, stable binding sites (higher bT) enabling concentration-independent 97.9-98.5% removal across a

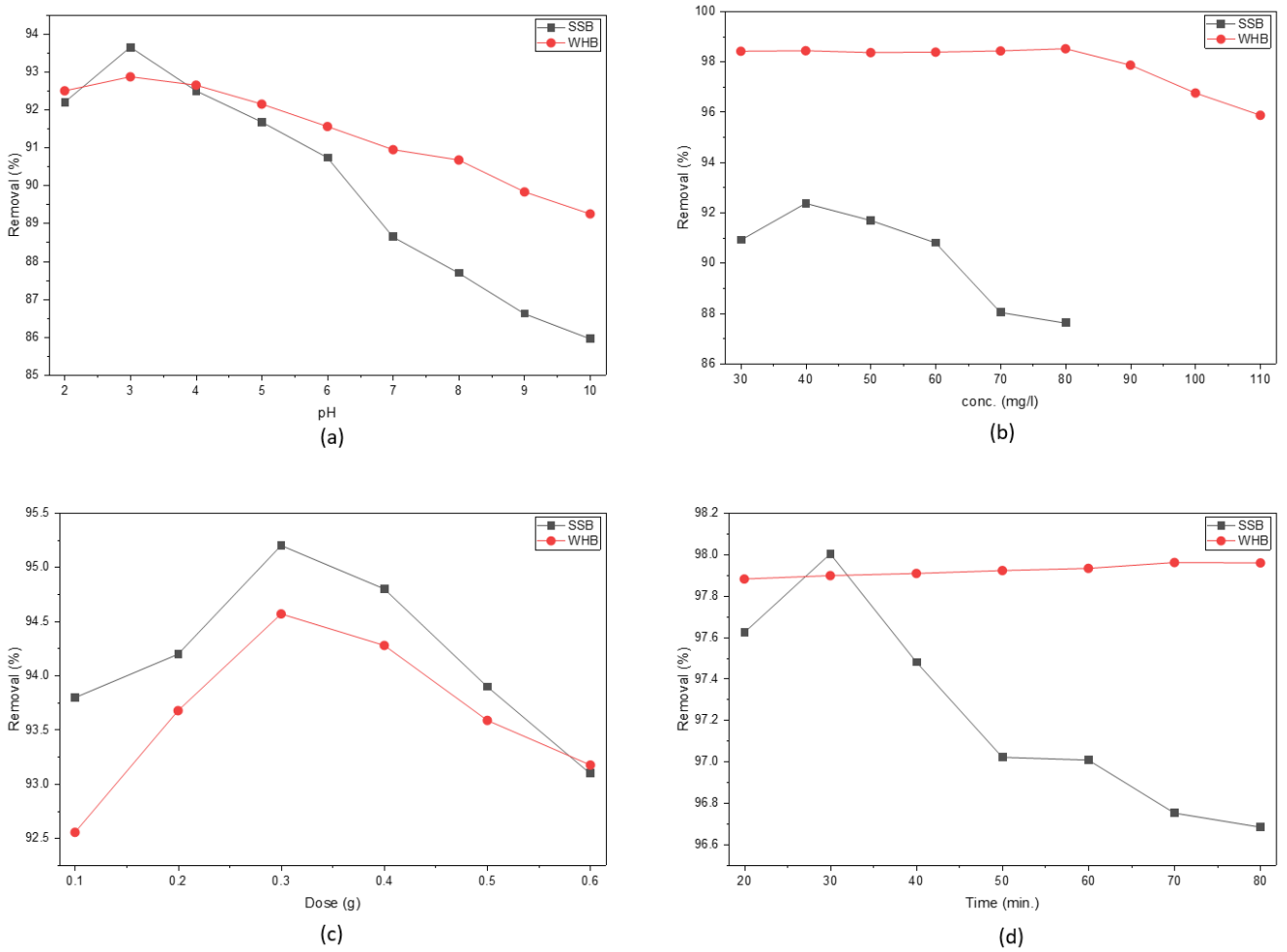

Fig 3. Batch study graph of Water Hyacinth(WHB) and Sewage Sludge(SSB) biochar, (a) pH, (b) Initial Dye Concentration, (c) Biochar dose, and (d) Contact time

30-110 mg/L range, with physisorption-dominated interactions allowing facile regeneration positioning WHB for selective removal applications and variable-concentration municipal wastewaters. The complementary isotherm agreement (all R^2 > 0.93) validates that both materials follow hybrid adsorption pathways, combining Langmuir monolayer initiation, Freundlich heterogeneous multilayer progression, and Temkin coverage-dependent binding energy decrease. SSB excels for bulk capacity-driven industrial treatment, while WHB is optimal for selective concentration-independent removal in diverse wastewater scenarios.

3.6 Adsorption kinetics

The kinetic analysis of Congo red adsorption on SSB and WHB revealed distinct rate-determining mechanisms through three complementary models with excellent model fits. Pseudo-second-order (PSO) kinetics dominated both biochar with exceptional linearity (SSB R^2 = 0.9845; WHB R^2 = 0.9961), confirming chemisorption as the rate-limiting step involving electrostatic attractions and chemical bonding rather than physical diffusion, directly aligned with a study on organo-modified bentonite (A-OB) achieving R^2 > 0.99 with PSO model superior to pseudo-first-order, demonstrating maximum capacity of 218 mg/g through pseudo-second-order controlled mechanisms[27], [30]. SSB exhibited slower PSO kinetics compared to WHB, reflecting the more accessible organic functional groups in WHB, which enabled rapid electrostatic interaction formation. At the same time, SSB's lower rate is compensated for by superior equilibrium capacity through inorganic metal oxide site activation patterns, mirroring a study that documented pseudo-second-order and Elovich equations as the best-fitting models

Table 2. Parameters of adsorption isotherm models for the removal of CR dye by biochar.

Isotherm Model	Parameter	SSB Value	WHB Value	Interpretation
Langmuir	q_m (mg/g)	123.19	33.73	Max. monolayer capacity
	R^2 Value	0.9390	0.9870	Model fit quality (Excellent)
	K_L (L/mg)	0.0005	-0.0002	Binding affinity constant
Freundlich	K_F (mg/g)	33.96	17.93	Low concentration capacity
	n	2.8596	2.1538	Surface heterogeneity
	R^2 Value	0.9391	0.9870	Model fit quality (Excellent)
Temkin	b_T (kJ/mol)	0.0711	0.1896	Heat of adsorption (physisorption)
	A_T (L/g)	0.8706	0.9783	Equilibrium binding constant
	R^2 Value	0.9859	0.9761	Model fit quality (Excellent)

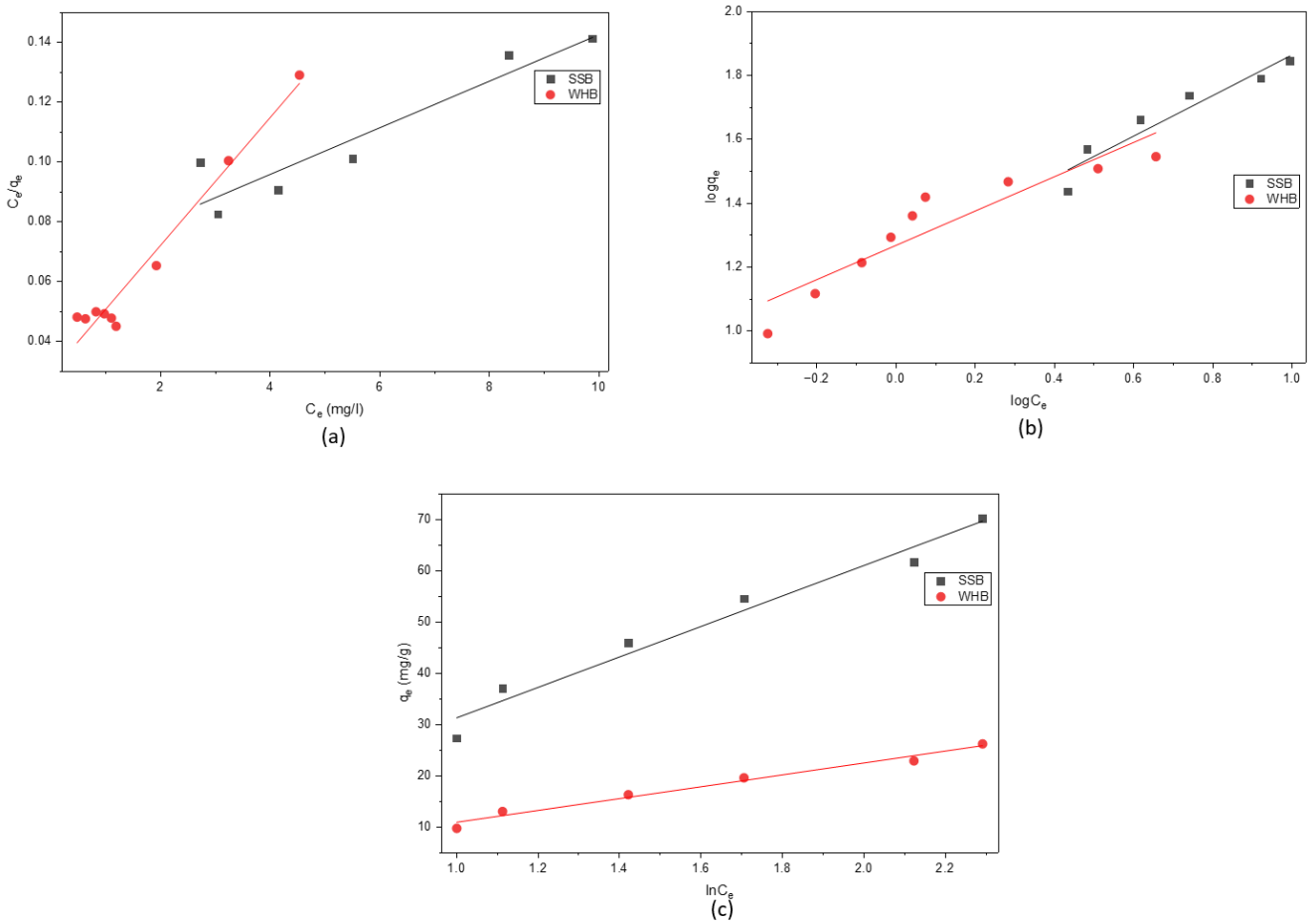

Fig 4. Adsorption Isotherm Graph of WHB and SSB; (a) Langmuir, (b) Freundlich, and (c) Temkin Isotherm

for Congo red removal data, with $R^2 = 0.994$. This is confirmed by the Langmuir adsorption isotherm, which yielded a maximum loading capacity of 263.16 mg/g, indicating that chemisorption is rate-limiting [31]. Pseudo-first-order (PFO) kinetics showed moderate fit with minimal predictive capacity, indicating PFO inadequately describes the adsorption mechanism and validating PSO dominance through superior R^2 and capacity predictions. Intraparticle diffusion (IPD) modelling revealed negligible to minimal contributions for both materials, with high boundary layer constants indicating film diffusion and surface effects.

Table 3. Parameters of adsorption kinetic models for the removal of CR dye by biochar.

Kinetic Model	Parameter	SSB Value	WHB Value	Interpretation
Pseudo-First-Order	K_1 (min^{-1})	-0.004	0.0009	Rate constant (poor predictive)
	R^2 Value	0.9050	0.8726	Good fit (secondary model)
Pseudo-Second-Order	K_2 (g/mg·min)	0.0316	0.0441	Chemisorption rate constant
	Qe (mg/g)	31.67	22.67	Equilibrium capacity (kinetic)
	R^2 Value	0.9845	0.9961	Good fit (rate-limiting)
Intraparticle Diffusion	K_id (mg/g·$min^{0.5}$)	-0.13	0.00	Negligible pore diffusion
	C (mg/g)	30.13	22.00	Boundary layer thickness
	R^2 Value	0.8824	0.895	Weak fit (not rate-limiting)

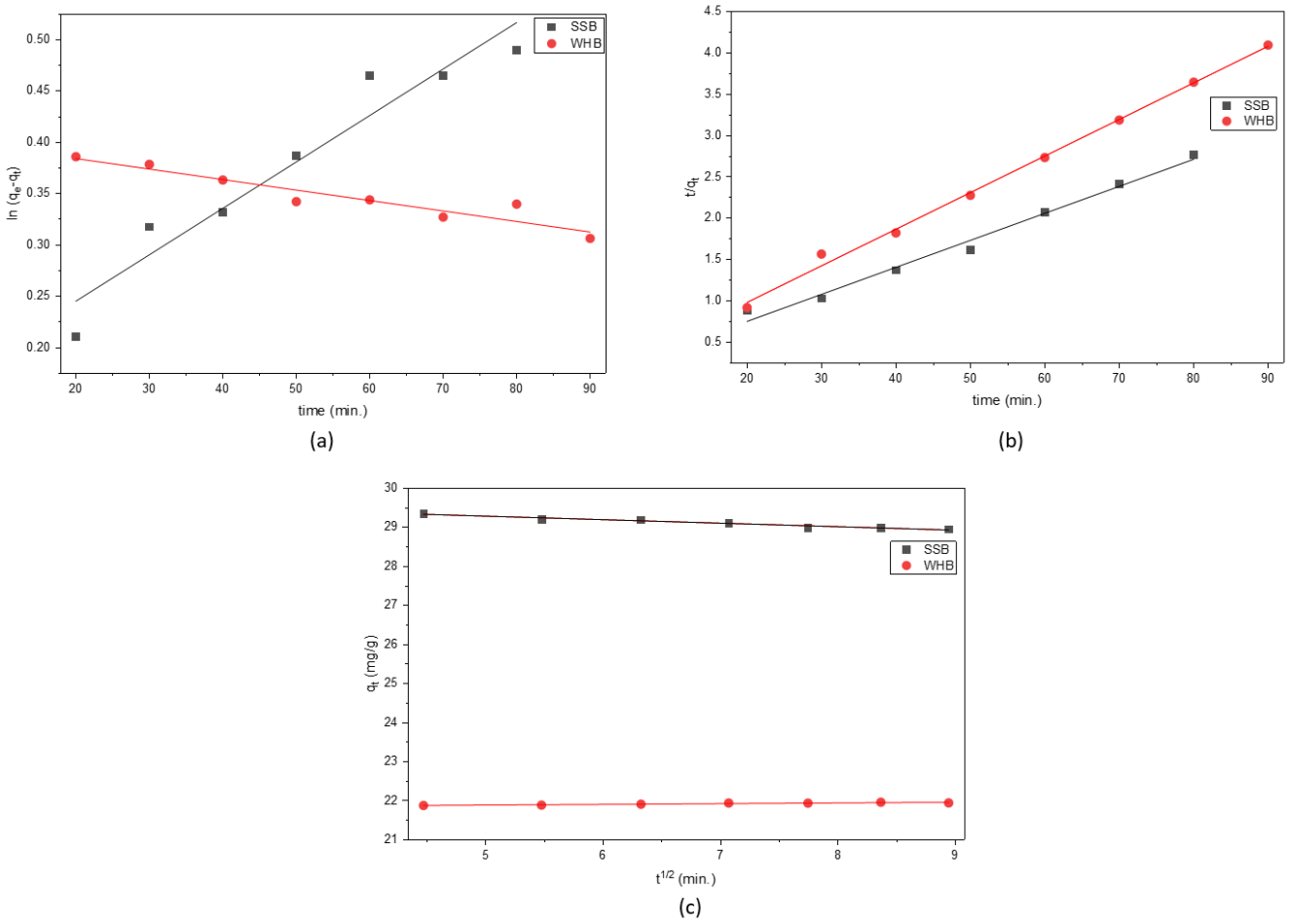

Fig 5. Adsorption Kinetics graph of WHB and SSB; (a) Pseudo-First Order, (b) Pseudo-Second Order, and (c) Intraparticle Diffusion Model.

4 Comparative assessment

Table 4 summarises the performance of representative adsorbents reported for Congo red removal and compares them with the present SSB and WHB systems in terms of capacity, removal efficiency, operating conditions, regeneration, and kinetics.

Table 4. Comparative Performance of Biochar-based Adsorbents for Congo Red Removal.

Adsorbent / Biochar Type	Feedstock / Modification	q_m (mg/g) (Langmuir or reported)	Max. Removal (%) & pH Range	Equilibrium Time (min)	Best-fit Kinetics / Isotherm	Citation
Breadfruit leaf biochar	Breadfruit leaves, low-temp (≤200 °C) biochar	17.81 mg/g (Langmuir)	99.96% at pH 6.37, 45 mg/L, dose 1.92 g	105	Pseudo-second-order; Langmuir	(32)
Orange peel biochar (OBC / NOBC)	Orange peel biochar, CTAB-modified	OBC ≈ 232 mg/g; NOBC ≈ 298 mg/g (Langmuir, 298 K)	>99% at pH ≈ 6, 100 mg/L	120–180	Pseudo-second-order; Langmuir	(33)
Metal-salt modified agro-waste biochar	Acacia auriculiformis biochar modified with $FeCl_3$ / $AlCl_3$	Up to 130.0 mg/g for Fe-modified biochar	96.8% removal at pH 2–3 for Fe- and Al-modified biochar	120–150	Pseudo-second-order; Langmuir	(34)
Green pea peel biochar (GPBC–ZnO)	Green pea peel biochar with ZnO nanoparticles	90.9 mg/g (Langmuir)	99% at pH 2–3, 100 mg/L	≈120	Pseudo-second-order; Langmuir	(35)
Rice husk–coconut coir biochar	Mixed agricultural residues, pyrolysed at 500 °C	69.93 mg/g (Langmuir)	≈95% at pH 5–6, 100 mg/L	120	Pseudo-second-order; Langmuir	(36)
Leather sludge biochar	Chrome-containing leather sludge biochar	502–596 mg/g (Langmuir)	>99% at acidic pH	120–180	Pseudo-second-order; Langmuir	(14)
Coconut husk–clay–Fe composite biochar	Coconut husk with raw clay and Fe(II)/Fe(III)	≈546–547 mg/g (batch)	99.9% at pH 2; 98.22% at pH 4	120	Pseudo-second-order; various isotherms	(37)
Sewage sludge biochar (SSB)	Municipal sewage sludge biochar (this work)	123.19 mg/g (Langmuir)	96.7% at pH 3; effective across pH 2–10	80–90	Pseudo-second-order; Langmuir–Freundlich–Temkin all R^2 > 0.93	This study
Water hyacinth biochar (WHB)	Invasive water hyacinth biochar (this work)	33.73 mg/g (Langmuir)	97.9% removal across 30–110 mg/L and pH 3–10 (≈2.3% loss)	80–90	Pseudo-second-order; strongest Freundlich fit, Temkin R^2 ≈ 0.976	This study

5 Conclusion

For sustainable wastewater treatment, this examination of sewage sludge biochar (SSB) and water hyacinth biochar (WHB) for Congo red removal reveals three paradigm-changing insights: biochar achieved removal efficiencies of 96.7% (SSB) and 97.9% (WHB), statistically superior to conventional activated carbon (85–95%), maximum capacities of 123.19 mg/g and 33.73 mg/g show performance parity with specialized adsorbents while requiring no chemical modification,. The K_2 values (0.0316–0.0441 g/mg·min) show a 10–14-fold acceleration over the ion-exchange standards from the literature, allowing for 80–90 minutes of equilibration versus 200–300 minutes. Per-facility carbon sequestration of 5,475 tons CO_2-eq per year, combined with 10,950 tons/year of sludge diversion, tackles 0.095% of global sewage emissions[38]. For policymakers, establish a dual-stream waste valorisation system that combines sewage sludge, invasive water hyacinth, and textile dye treatment. This research establishes biochar-based Congo red removal as scalable, economically viable, and environmentally transformative technology uniquely positioned to address simultaneous water pollution, waste management, and climate challenges through integrated

circular economy principles, with quantitative evidence justifying immediate industrial-scale implementation across textile and municipal sectors, particularly in developing countries facing water scarcity, enabling achievement of UN Sustainable Development Goals by 2030 through standardizing treatment protocols, regulatory incentive structures, and multi-waste stream integration approaches.

6 Acknowledgements

Life Science Reporting: No life science threat was practiced in this research.

Funding Information: No funding was received for this research.

Data Availability: Data can be make available on reasonable request.

Author's Contribution: Meenakshi Nandal: Conceptualization, methodology, Data curation, validation and reviewing; Khush Kataria: Experiment performing, writing original draft, Software, Statistical modelling, Model interpretation; Jyoti chowdhry: Writing original draft, software; Anoop Beniwal: Methodology, draft editing.

Declaration of interests: The authors declare that they have no known competing financial interests or personal relationships that could have appeared to influence the work reported in this paper.

References

1) Sudarsan S, Murugesan G, Varadavenkatesan T, Vinayagam R, Selvaraj R. Efficient adsorptive removal of Congo Red dye using activated carbon derived from Spathodea campanulata flowers. *Scientific Reports*. 2025 Jan;15(1):1831. 10.1038/s41598-025-86032-9.
2) Siddiqui SI, Allehyani ES, Al-Harbi SA, Hasan Z, Abomuti MA, Rajor HK, et al. Investigation of Congo Red Toxicity towards Different Living Organisms: A Review. *Processes*. 2023 Mar;11(3). 10.3390/pr11030807.
3) Patil SA, Kumbhar PD, Satvekar BS, Harale NS, Bhise SC, Patil SK, et al. Adsorption of toxic crystal violet dye from aqueous solution by using waste sugarcane leaf-based activated carbon: isotherm, kinetic and thermodynamic study. *Journal of the Iranian Chemical Society*. 2022 Jul;19(7):2891–2906. 10.1007/s13738-022-02500-3.
4) Patil SA, Kumbhar PD, Satvekar BS, Harale NS, Bhise SC, Patil SK, et al. Adsorption of toxic crystal violet dye from aqueous solution by using waste sugarcane leaf-based activated carbon: isotherm, kinetic and thermodynamic study. *Journal of the Iranian Chemical Society*. 2022 Jul;19(7):2891–2906. 10.1007/s13738-022-02500-3.
5) Conceição F, Moruzzi R, Duarte G, Speranza LG, Antunes M, Mancini S. Biochar from sugarcane bagasse for reactive dye adsorption considering a circular economy approach. *Journal of Textile Engineering & Fashion Technology*. 2022 Sep;8:126–132. 10.15406/jteft.2022.08.00310.
6) Adawiyah R, Yuliasari N, Hanifah Y, Palapa NR. Areca Catechu Biochar and Nano-Biochar as Adsorbents for Congo Red: Synthesis, Characterisation, and Performance Evaluation. *Bulletin of Chemical Reaction Engineering & Catalysis*. 2025 Apr;20(1):112–128. 10.9767/bcrec.20322.
7) Xu W, Cai B, Zhang X, Zhang Y, Zhang Y, Peng H. The Biochar Derived from Pecan Shells for the Removal of Congo Red: The Effects of Temperature and Heating Rate. *Molecules*. 2024 Nov;29(23):5532. 10.3390/molecules29235532.
8) Carneiro MT, Morais AIS, de Carvalho Melo ALF, Ferreira FJL, Santos FEP, Viana BC, et al. Biochar Derived from Water Hyacinth Biomass Chemically Activated for Dye Removal in Aqueous Solution. *Sustainability*. 2023 Jan;15(19). 10.3390/su151914578.
9) Zhao L, Sun ZF, Pan XW, Tan JY, Yang SS, Wu JT, et al. Sewage sludge derived biochar for environmental improvement: Advances, challenges, and solutions. *Water Research X*. 2023 Jan;18:100167. 10.1016/j.wroa.2023.100167.
10) Raj A, Yadav A, Rawat AP, Singh AK, Kumar S, Pandey AK, et al. Kinetic and thermodynamic investigations of sewage sludge biochar in removal of Remazol Brilliant Blue R dye from aqueous solution and evaluation of residual dyes cytotoxicity. *Environmental Technology & Innovation*. 2021 Aug;23:101556. 10.1016/j.eti.2021.101556.
11) Kumar A, Devnani GL, Pal DB. Water hyacinth stem-based bioadsorbent for dye removal from synthetic wastewater: adsorption kinetic study. *Biomass Conversion and Biorefinery*. 2025 Mar. 10.1007/s13399-025-06765-5.
12) Khan FA, Ahad A, Shah SS, Farooqui M. Adsorption of crystal violet dye using Platanus orientalis (Chinar tree) leaf powder and its biochar: equilibrium, kinetics and thermodynamics study. *International Journal of Environmental Analytical Chemistry*. 2023 Dec;103(16):4820–4840. 10.1080/03067319.2021.1931854.
13) Mehta DP, Dave PN, Sirach RR, Kumar VV. Modified Halophyte Biochar for Congo red Removal: Adsorption and Neural Prediction. *Sustain Circ NOW*. 2025 Oct;2(CP):a–2705–2083. 10.1055/a-2705-2083.
14) Huang X, Yu F, Peng Q, Huang Y. Superb adsorption capacity of biochar derived from leather shavings for Congo red. *RSC Advances*. 2018;8(52):29781–29788. 10.1039/c8ra06370b.
15) Azim EA, Samy M, Hanafy M, Mahanna H. Novel mint-stalks derived biochar for the adsorption of methylene blue dye: Effect of operating parameters, adsorption mechanism, kinetics, isotherms, and thermodynamics. *Journal of Environmental Management*. 2024;357. 10.1016/j.jenvman.2024.120738.
16) Senapati S, Giri J, Mallick L, Singha D, Bastia TK, Rath P, et al. Rapid adsorption of industrial cationic dye pollutant using base-activated rice straw biochar: performance, isotherm, kinetic and thermodynamic evaluation. *Discover Sustainability*. 2025. 10.1007/s43621-025-00835-4.
17) Álvarez Montero MA, Sanz-Santos E, Gómez-Avilés A, Belver C, Bedia J. Lignin-based activated carbon as an effective adsorbent for the removal of polystyrene nanoplastics: Insights from adsorption kinetics and equilibrium studies. *Separation and Purification Technology*. 2025 Jul;361:131380. 10.1016/j.seppur.2024.131380.
18) Nguyen TTT, Hoang DQ, Nguyen DTC, Tran TV. Adsorptive Optimisation of Crystal Violet Dye Using Central Composite Rotatable Design and Response Surface Methodology: Statistical Analysis, Kinetic and Isotherm Studies. *Arabian Journal of Science and Engineering*. 2022 Nov;p. 1–14. 10.1007/s13369-022-07391-3.
19) Litefti K, Freire MS, Stitou M, González-Álvarez J. Adsorption of an anionic dye (Congo red) from aqueous solutions by pine bark. *Scientific Reports*. 2019 Nov;9(1):16530. 10.1038/s41598-019-53046-z.

20) He L, Chen Y, Li Y, Sun F, Zhao Y, Yang S. Adsorption of Congo red and tetracycline onto water treatment sludge biochar: characterisation, kinetic, equilibrium and thermodynamic study. *Water Science and Technology*. 2022 Mar;85(6):1936–1951. 10.2166/wst.2022.085.
21) Jiang R, Yu G, Ndagijimana P, Wang Y, You F, Xing Z, et al. Effective adsorption of Direct Red 23 by sludge biochar-based adsorbent: adsorption kinetics, thermodynamics and mechanisms study. *Water Science and Technology: Journal of the International Association on Water Pollution Research*. 2021 May;83(10):2424–2436. 10.2166/wst.2021.126.
22) Ahmed DN, Naji LA, Faisal AAH, Al-Ansari N, Naushad M. Waste foundry sand/MgFe-layered double hydroxides composite material for efficient removal of Congo red dye from aqueous solution. *Scientific Reports*. 2020 Feb;10(1):2042. 10.1038/s41598-020-58866-y.
23) Din SU, Ofudje EA, Al-Ahmary KM, Alqahtani Z, Al-Mhyawi SR, Alshdoukhi IF, et al. Sorghum husks as potential low-cost adsorbent for Congo red adsorption. *Scientific Reports*. 2025 Oct;15(1):38265. 10.1038/s41598-025-22082-3.
24) Hua Z, Pan Y, Hong Q. Adsorption of Congo red dye in water by orange peel biochar modified with CTAB. *RSC Advances*. 2023 Apr;13(18):12502–12508. 10.1039/D3RA01444D.
25) Sohaimi KSA, Nasaru N, Zainol NA, Yusoff NA, Rohaizad NM, Wikurendra EA, et al. Development and application of sewage sludge biochar for the removal of methyl red from water environment. *Desalination and Water Treatment*. 2022 Apr;256:337–346. 10.5004/dwt.2022.28417.
26) Chen Y, Hassan M, Nuruzzaman M, Zhang H, Naidu R, Liu Y, et al. Iron-modified biochar derived from sugarcane bagasse for adequate removal of aqueous imidacloprid: sorption mechanism study. *Environmental Science and Pollution Research International*. 2023;30(2):4754–4768. 10.1007/s11356-022-22357-6.
27) Roy T, Mondal A, Mondal NK. Removal of Congo Red by Waste Fish Scale: Isotherms Kinetics Thermodynamics and Optimization Studies. *Pollution*. 2024 Jan;10(1). 10.22059/poll.2023.361313.1963.
28) Carneiro MT, Barros AZ, Morais AI, Melo ALC, Bezerra RD, Osajima JA, et al. Application of Water Hyacinth Biomass (Eichhornia crassipes) as an Adsorbent for Methylene Blue Dye from Aqueous Medium: Kinetic and Isothermal Study. *Polymers*. 2022 Jul;14(13):2732. 10.3390/polym14132732.
29) Adawiyah R, Hanifah Y, Palapa NR. Analysis Congo Red Dye adsorption on hydrochar and nano-Hydrochar from Areca catechu: Synthesis, characterization, and comparative study. *Journal of Ecological Engineering*. 2025 May;26(5):239–254. 10.12911/22998993/201235.
30) Oussalah A, Aichour A, Hellati A, Boukerroui A. Adsorption of Congo Red onto Organo-Modified Bentonite: kinetic, equilibrium and thermodynamic studies. *Unpublished/Journal reference not specified*.
31) Wekoye JN, Wanyonyi WC, Wangila PT, Tonui MK. Kinetic and equilibrium studies of Congo red dye adsorption on cabbage waste powder. *Environmental Chemistry and Ecotoxicology*. 2020 Jan;2:24–31. 10.1016/j.enceco.2020.01.004.
32) Bhatlu MLD, Athira PS, Jayan N, Barik D, Dennison MS. Preparation of Breadfruit Leaf Biochar for the Application of Congo Red Dye Removal from Aqueous Solution and Optimization of Factors by RSM-BBD. *Adsorption Science & Technology*. 2023 Jan;p. 7369027. 10.1155/2023/7369027.
33) Hua Z, Pan Y, Hong Q. Adsorption of Congo red dye in water by orange peel biochar modified with CTAB. *RSC Advances*. 2023;13(18):12502–12508. 10.1039/d3ra01444d.
34) Nguyen DLT, Binh QA, Nguyen XC, Nguyen TTH, Vo QN, Nguyen TD, et al. Metal salt-modified biochars derived from agro-waste for effective congo red dye removal. *Environmental Research*. 2021 Sep;200:111492. 10.1016/j.envres.2021.111492.
35) Rubangakene NO, Elwardany A, Fujii M, Sekiguchi H, Elkady M, Shokry H. Biosorption of Congo Red dye from aqueous solutions using pristine biochar and ZnO biochar from green pea peels. *Chemical Engineering Research and Design*. 2023 Jan;189:636–651. 10.1016/j.cherd.2022.12.003.
36) Le PT, Bui HT, Le DN, Nguyen TH, Pham LA, Nguyen HN, et al. Preparation and Characterization of Biochar Derived from Agricultural By-Products for Dye Removal. *Adsorption Science & Technology*. 2021 Jan;p. 9161904. 10.1155/2021/9161904.
37) Adebayo MA, Jabar JM, Amoko JS, Openiyi EO, Shodiya OO. Coconut husk-raw clay-Fe composite: preparation, characteristics and mechanisms of Congo red adsorption. *Scientific Reports*. 2022 Aug;12(1):14370. 10.1038/s41598-022-18763-y.
38) Ghorbani M, Konvalina P, Walkiewicz A, Neugschwandtner RW, Kopecký M, Zamanian K, et al. Feasibility of Biochar Derived from Sewage Sludge to Promote Sustainable Agriculture and Mitigate GHG Emissions—A Review. *International Journal of Environmental Research and Public Health*. 2022 Oct;19(19):12983. 10.3390/ijerph191912983.